



Towards efficient Monte Carlo N-Particle simulation of a positron emission tomography (PET) via source volume definition

Nazreen Waeleh^{a,b,*}, M. Iqbal Saripan^a, Marianie Musarudin^c, Fathinul Fikri Ahmad Saad^d, Syamsiah Mashohor^a, Suhairul Hashim^e

^a Faculty of Engineering, Universiti Putra Malaysia, 43400 Serdang, Selangor, Malaysia

^b Faculty of Electronic and Computer Engineering, Universiti Teknikal Malaysia Melaka (UTeM), 76100 Durian Tunggal, Melaka, Malaysia

^c School of Health Sciences, Health Campus, Universiti Sains Malaysia, 16150 Kubang Kerian, Kelantan, Malaysia

^d Centre for Diagnostic Nuclear Imaging, Universiti Putra Malaysia, 43400 Serdang, Selangor, Malaysia

^e Department of Physics, Universiti Teknologi Malaysia, 81310, Johor Bahru, Malaysia

ARTICLE INFO

Keywords:

Positron emission tomography
Radiation source
Variance reduction

ABSTRACT

Monte Carlo N-Particle (MCNP) simulation has been extensively proven in nuclear medicine imaging systems, most notably in designing and optimizing new medical imaging tools. It enables more complicated geometries and the simulation of particles passing through and interacting with materials. However, a relatively long simulation time is a drawback of Monte Carlo simulation, mainly when complex geometry exists. The current study presents an alternative variance reduction technique for a modeled positron emission tomography (PET) camera by reducing the height of the source volume definition while maintaining the geometry of the simulated model. The National Electrical Manufacturers Association (NEMA) of the International Electrotechnical Commission (IEC) PET's phantom was used with a 1 cm diameter and 7 cm height of line source placed in the middle. The first geometry was fully filled the line source with 0.50 mCi radioactivity. In contrast, the second geometry decreased the source definition to 2.4 cm in height, covering 1 cm above and below the sub-block detector level. The source volume definition approach led to a 71% reduction in the total photons to be simulated. Results showed that the proposed variance reduction strategy could produce spatial resolution as precise as fully filled geometry and sped up the simulation time by approximately 65%. Hence, this strategy can be utilized for further PET optimizing simulation studies.

1. Introduction

Nuclear medicine imaging, a medical speciality which assists in diagnosis and capable of prescribing subsequent treatment of a disease in its early progression, examines a patient's radioactivity distribution images. In the procedure, emitting photons from a patient's body are captured by external scintillation detectors before converting them into signals (Yanagida, 2018). The acquired signals subsequently determine the quality of medical images generated, thus compelling the need for crucial selection of a good scintillation material (Xie et al., 2020). The most commonly considered elements for crystal scintillator are materials with high densities and attenuation coefficients as these materials could effectively stop the penetration of high-energy photons (Raylman et al., 2022). To date, sodium iodide (NaI), bismuth germanium oxide (BGO), lutetium oxyorthosilicate (LSO) and lutetium yttrium

oxyorthosilicate (LYSO) are among the inorganic crystals commonly used to collect the deposition of high-energy gamma photons for positron emission tomography (PET) imaging (Tan et al., 2020). PET has become a well-established and widely utilized imaging modality in both clinical and preclinical settings due to improvement in scintillation material. The configuration of full-ring detectors in PET have allowed for fast dynamic scans and extensive body-coverage scanning ability (Beyer et al., 2020).

In the field of medical radiation physics, the Monte Carlo simulation, developed for precise designing, optimizing, and understanding of new emission tomography systems for nuclear-based imaging has been regarded as the most accurate calculation engine currently available (Salvadori et al., 2020). In essence, PET calculates the distribution of particle transport involving both primary and scattered photons in a scattering medium using this platform. Researchers generally model

* Corresponding author. Faculty of Electronic and Computer Engineering, Universiti Teknikal Malaysia Melaka (UTeM), 76100, Durian Tunggal, Melaka, Malaysia.
E-mail address: nazreen@utem.edu.my (N. Waeleh).

interactions of realistic photon between an object and a PET detector while acquiring detailed reference activity and attenuation distributions. These information are important in image reconstruction procedures, in which adequate corrections can be implemented to the detected gamma rays to compensate the attenuation caused by different body tissues. Two types of corrections that are usually implemented in PET image reconstruction are attenuation and scatter corrections, both of which degrade the quality of PET imaging. However, due to body environment, attenuation correction is generally more dominant than scatter correction (Martinez-Möller and Nekolla, 2012). Since PET images need to maintain a certain level of diagnostic accuracy, past studies have demonstrated that their quality can be regulated prior to, during, or after PET simulations. To accomplish this objective, a simulation of particle transport that accurately mimics the real system is required. To date, among the available Monte Carlo codes, a Monte Carlo N-Particle (MCNP) has been reported to have been widely used in studies modeling particle transports in detector response calculations (Goorley et al., 2016).

Studies have shown that MCNP approach in radiation physics is limited by the fact that it is, by nature, an extremely time-consuming proposition (Pfaehler et al., 2018). The length of time needed to complete a computation has been reported to be proportional to a number of factors including the number, energy, types of particles to be simulated, as well as the medium through which they are transported. Generally, tracking of hundreds, thousands, or even millions of particles is required in order to acquire reliable statistics (Loudos, 2007). In view of this, development of more sophisticated computers equipped with the ability to perform simultaneous calculations has materialized as an alternate method for achieving practical simulation time. In a successful MCNP simulation, while precision is not the only element that matters; computing time is also of utmost importance. As an alternative, non-imaging methodological advancement called variance reduction techniques (VRTs) have been developed to improve detector modeling as well as to significantly reduce computing time (Sarrut et al., 2021). The VRT can be defined as the process of lowering the variance of MCNP tallies or decreasing the amount of time required for each particle simulation. Numerous VRTs for Monte Carlo simulations are available, while Woodcock tracking has been quoted as a suitable entity for emission tomography when working with an analytical or neural network models to track particles. These methods have the potential of significant acceleration, depending on a number of factors, such as simulation configurations (Wang et al., 2016).

MCNP has four distinguishable groups of VRTs, covering from simple to complex. The simplest is truncation, which speeds up calculations by removing irrelevant phases and making the MCNP model simpler. An elemental example is truncating or shortening a geometry, which bypasses the outer parts of that geometry. MCNP offers two types of truncations: energy and time, both of which conserve time by terminating particles whose energy and duration are irrelevant. MCNP uses particle-splitting, as well as Russian roulette in regulating the number of samples for a population control (Mohammed et al., 2016). Weight adjustment is applied to counter-balance samples of low weight tracked in essential places and to offset high weight in insignificant regions. In a previous study, Shultis and Faw (2011) cited that VRTs changed the statistical sampling to increase the number of tallies per particle by directing the particles into specific regions of phase spaces, such as time, energy, position, or collision type. Among the partially predetermined methods, the most complex VRTs have been reported using predetermined-like approaches to predict or manipulate random sequences. In MCNP, use of point detectors, DXTRAN and correlated sampling have been cited.

In the present study, MCNP Version 5 (MCNP5) algorithm was used to model Siemens Biograph TruePoint PET/CT scanner. All output information on annihilation photons occurring in PET system were located in a file known as particle track output card (PTRAC). Since PTRAC prevents simulation via a computer cluster (Saeed et al., 2016), the

present study developed a new variance in reduction strategy. The strategy was specifically tailored to the geometry of the modeled PET scan for accelerating simulation. Two MCNP simulation geometries were investigated, with VRT applied to Geometry 2. The implementation of these two distinct geometries was based on the volumetric adjustment of radioactivity in the input card. The approach produced positive results by significantly enhancing computing efficiency while preserving accuracy.

2. Materials and methods

The study was divided into three parts: simulation setup, variance reduction, and evaluation. Firstly, a PET camera and phantom geometry capable of reproducing PET imaging process, was developed. Subsequently, a discussion on how the suggested PET geometry incorporated VRT including materials utilized and number of particles in a prescribed volume was carried out. In the final procedure, image performance was evaluated.

2.1. Simulation setup

For each MCNP simulation, an input file was created. Each simulation contained information on geometry, materials and sources to be used, as well as the desired outcome. The geometry of the main component of the simulated PET scanner was designed to be close to the actual, and subsequently, the F8 tally, which provided information on the energy deposition, was selected. Literature has it that precision is necessary to run a simulation that performs identically to a natural PET system. The PET scan model developed in the present study was based on Siemens Biograph TruePoint PET/CT scanner, featuring a phantom geometry that closely resembled NEMA IEC PET phantom design (Waeleh et al., 2021). The ring detector was the primary and most critical component of the PET system. It was designed with a circular PET tomograph of 84.2 cm in diameter and with 48 independent LSO block detectors with each scintillation crystal block being subdivided into 13 smaller blocks, each measuring 0.4 cm × 0.4 cm × 2.0 cm in size, generating a total of 624 crystal elements. In the actual PET detector block configurations, there are thirty-nine rings detectors for a full design representing the width of PET ring by approximately 15.6 cm. In the present study, a single-ring layer with a width of 0.4 cm to initiate image formation, was used (Fig. 1a). It can be considered as an appropriate procedure as the image formation was evaluated in a single-slice image. The model was validated with one being generated from actual experiment conducted at the Center for Diagnostic Nuclear Imaging (CDNI) at Universiti Putra Malaysia (UPM) (Waeleh et al., 2021). Both the simulated and experimental results were consistent, suggesting that it is possible to utilize the developed model for PET studies.

2.2. Variance reduction

In the model presently developed, a variance reduction was empirically defined with a suitable and practical strategy implemented in the modeled PET geometry. The shape of the simulated model was preserved to maintain the photon's physical interaction characteristics. Two sets of simulations were conducted to confirm the efficiency of the proposed VRT. A line source of 1 cm in diameter and 7 cm in height was positioned at the center of the phantom. In Geometry 1 (Fig. 1b), the line source was filled with 0.5 mCi radioactivity. In Geometry 2 (Fig. 1c), the definition of the source was reduced to 2.4 cm high, covering 1 cm above and below the level of the sub-block detector. The purpose of reducing the height of the source definition was to shorten the duration of simulation. The reduction aided the simulation by utilizing fewer photons making the approach a proposed variance reduction strategy. The number of photons to be emitted throughout the simulation was calculated based on the integration rate of the corresponding source activity (A mCi) and the acquisition time (t second), as shown in (1) (Musarudin

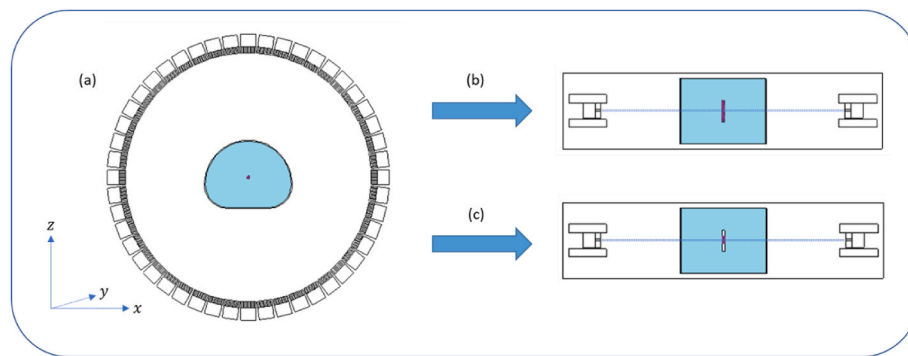


Fig. 1. Geometrical structures of PET camera based on MCNP, viewed in (a) xz direction, (b) xy direction (Geometry 1) and (c) xy direction (Geometry 2).

et al., 2015).

$$nps = A \times 3.7 \times 10^7 \times t \quad (1)$$

In the first part of the study, the total number of photons required was 2.220×10^9 , which was the result of 0.5 mCi of radioactivity and a scanning time of 120 s. A starting value of 0.5 mCi was selected for testing the proposed VRT, as this approach is to be used in future studies to analyse experiments requiring greater amount of radioactivity. By introducing a source volume-reduction definition, the present study reduced the total number of photons by approximately 71%, which is equivalent to 7.611×10^8 . This number was deemed sufficient for MCNP simulation in order to achieve adequate statistical uncertainty (Holdsworth et al., 2001). The accuracy of the strategy was compared with spatial resolution, while the efficiency was determined by comparing the total time required to complete each simulation directly. To determine the spatial resolution of a PET system, reconstructing a point source scan and calculating the full width at half maximum (FWHM) along the principal directions are necessary. The determination of spatial resolution has been cited as an essential parameter for performance characterization in PET systems (Gong et al., 2016).

2.3. Evaluation on performance of imaging output

Within the context of this investigation, a sizable output file was generated when a substantial number of photons were considered. Using a PTRAC card, the output file was subsequently filtered only to record data required for the present study. The PTRAC file recorded prediction and activity of each annihilation photon from the time it was produced. PET primary data consist of forecast information about a patient, while the sinogram matrix is a collection of projections from 0 to 360°. The data were corrected for attenuation before they transformed into an image using image reconstruction, which in turn, transformed the forecast count to an image that accurately depicted the distribution of radioactivity throughout the patient's body. The entirety of the image reconstruction procedure was performed using MATLAB, a high-level programming language. At present, two fundamental approaches to image reconstruction are analytical and iterative methods. In the present study, the analytic reconstruction algorithm, commonly referred to as filtered back-projection (FBP) was used. The FBP is widely known for having quick processing time while maintaining an acceptable image quality (Dietze et al., 2019; Dolmatova et al., 2020). Together with FBP, a Hann filter was utilized. The study consequently established a point spread function image by imaging a line source with a PET scanner. The FWHM of the intensity profile distinctively displayed across the center of each small source image was used to determine the spatial resolution, calculated using a Gaussian fitted profile (Zhao et al., 2022).

3. Results and discussion

Variance reduction strategies are essential components in any Monte

Carlo algorithm and generally vary based on application and geometry. Hence, numerous variance reduction strategies have been proposed to reduce simulation duration and increase precision. Variance reduction is generally included in MCNP5 but deemed inapplicable for developed PET modeling. A narrower source width has been proposed to lower the overall number of photons necessary for simulation of developed PET. In the present study, reduction was made after meticulous assessments on the activity of tumor volume and the detectors' position. For validity of the proposed method, it was compared with simulations of full-width source modeling. The accuracy was determined by comparing the spatial resolution of two generated images. Its efficiency was established by comparing the total time required to complete each simulation.

The imitative representation of spatial resolution presented in Fig. 2 was derived from Geometry 1 and Geometry 2. This resolution was generated from the FWHM calculation for 1 cm diameter of line source scanning in full- and reduced-width simulations, respectively. For full-width simulation depicted in Fig. 2a, its spatial resolution was 3.76 pixels, whereas the reduced-width simulation represented in Fig. 2b had a pixel size of 3.83, generating a difference of less than 0.1 pixel suggesting that these two geometries are in agreement. The data demonstrated that simulations using Geometry 2 modeling could reproduce results similar to using Geometry 1. The favorable performance was due to the modeling of a single ring detector and the production of a 2-D plane image. Reducing activity in source height had no discernible effect on the reconstruction of image's accuracy because the height of the defined source covered the ring detector's height. The application of 0.5 mCi demonstrated that simulation accuracy could be maintained (Waeleh et al., 2021), while variance reduction had no effect on accuracy. The study finds that it is absolutely necessary to accomplish this accuracy before attempting to apply the model to subsequent PET investigations involving higher radioactive dose.

The high computational cost in simulation has been cited to be typically accelerated via parallel computing (Okubo et al., 2017). In the present study, this simulation cannot be implemented due to output card limitations. Simulations were executed serially on a 3.20 GHz-core Intel (R) Xeon(R) Gold 6134 central processing unit (CPU). For this specific attribute, the VRT contributed significantly toward shortening the computational time. Fig. 3 shows that it took a total of 46 days for the simulation to run completely all the histories using Geometry 1. When VRT was implemented, 30 days were saved, allowing Geometry 2 to complete the simulation in 16 days, suggesting that narrowing source height accelerated the simulation of Geometry 2 by about 65%. The results were as expected while both sources of volume and photons decreased simultaneously, given the computation time in MCNP was proportional to the total number of particles generated (Zoubair et al., 2013). Due to this, the overall amount of time needed to run all of the photons was drastically reduced, which was regarded as a successful outcome. This also indicates the effectiveness of the proposed strategy in decreasing CPU time without altering the nature of the problem, thus presenting significant cost savings, as future studies stand in need of

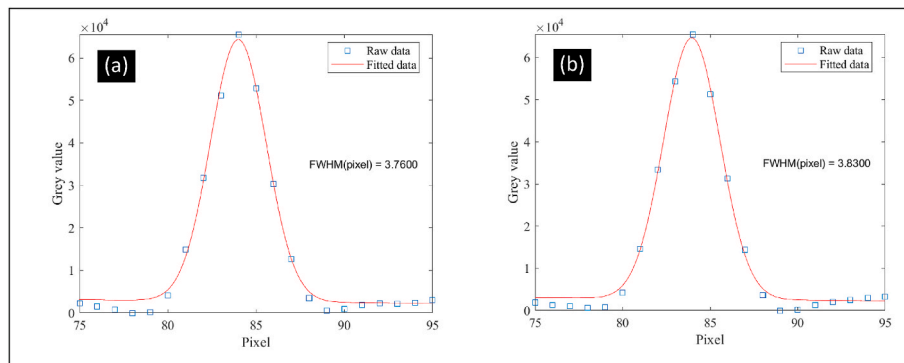


Fig. 2. Full width at half maximum (FWHM) for (a) Geometry 1 and (b) Geometry 2.

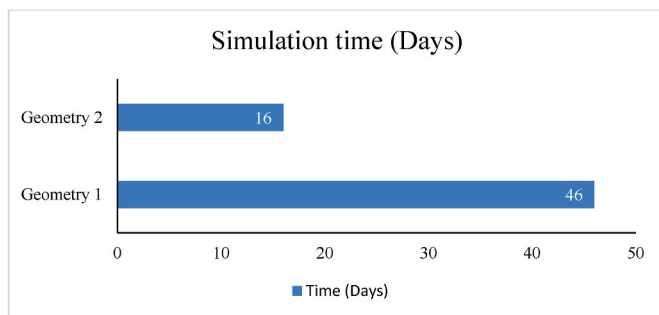


Fig. 3. Completed simulation time for Geometry 1 and Geometry 2.

more complex simulations using the same model.

4. Conclusion

This paper discusses a procedure for reducing variance on the basis of definition of a compatible source volume with modeled PET scanner. The results confirmed that the suggested variance reduction strategy had enabled Geometry 2 to replicate the results as precisely as Geometry 1 modeling while incurring less computing expenses. The remarkable agreement between these two geometry calculations demonstrated the practicability and validity of the proposed method. The proposed VRT developed in the present study was intended to contribute significantly to existing empirical literature and to offer insight for further research on tomography studies since it improves efficiency by approximately a factor of three, which could result in significant reduction in the amount of computational effort involving a greater number of treated particles.

CRediT authorship contribution statement

Nazreen Waeleh: Writing – review & editing, Writing – original draft, Visualization, Validation, Project administration, Methodology, Investigation, Formal analysis, Data curation, Conceptualization. **M. Iqbal Saripan:** Writing – review & editing, Visualization, Validation, Supervision, Software, Resources, Methodology, Funding acquisition, Conceptualization. **Marianie Musarudin:** Writing – review & editing, Visualization, Validation, Supervision, Methodology, Conceptualization. **Fathinul Fikri Ahmad Saad:** Writing – review & editing, Validation, Supervision, Methodology, Conceptualization. **Syamsiah Mashohor:** Writing – review & editing, Visualization, Validation, Supervision, Methodology, Conceptualization. **Suhairul Hashim:** Visualization, Writing – review & editing.

Declaration of competing interest

The authors declare that they have no known competing financial

interests or personal relationships that could have appeared to influence the work reported in this paper.

Data availability

The data that has been used is confidential.

Acknowledgements

Universiti Putra Malaysia funded this study under Grant no. 9662900. The first author would like to warmly thank Universiti Teknikal Malaysia Melaka and the Ministry of Higher Education Malaysia for the doctoral study scholarship award.

References

- Beyer, T., Bidaut, L., Dickson, J., Kachelriess, M., Kiessling, F., Leitgeb, R., Ma, J., Shiyam Sundar, L.K., Theek, B., Mawlawi, O., 2020. What scans we will read: imaging instrumentation trends in clinical oncology. *Cancer Imag.* 20 (1), 1–38. <https://doi.org/10.1186/s40644-020-00312-3>.
- Dietze, M.M.A., Branderhorst, W., Kunnen, B., Viergever, M.A., de Jong, H.W.A.M., 2019. Accelerated SPECT image reconstruction with FBP and an image enhancement convolutional neural network. *EJNMMI Physics* 6 (1). <https://doi.org/10.1186/s40658-019-0252-0>.
- Dolmatova, A., Chukalina, M., Nikolaev, D., 2020. Accelerated FBP for computed tomography image reconstruction. In: *International Conference on Image Processing. ICIP*, pp. 3030–3034.
- Gong, K., Cherry, S.R., Qi, J., 2016. On the assessment of spatial resolution of PET systems with iterative image reconstruction. *Phys. Med. Biol.* 61 (5), N193–N202. <https://doi.org/10.1088/0031-9155/61/5/N193>.
- Goorley, T., James, M., Booth, T., Brown, F., Bull, J., Cox, L.J., Durkee, J., Elson, J., Fensin, M., Forster, R.A., Hendricks, J., Hughes, H.G., Johns, R., Kiedrowski, B., Martz, R., Mashnik, S., McKinney, G., Pelowitz, D., Prael, R., et al., 2016. Features of MCNP6. *Ann. Nucl. Energy* 87, 772–783. <https://doi.org/10.1016/j.anucene.2015.02.020>.
- Holdsworth, C.H., Levin, C.S., Farquhar, T.H., Dahlbom, M., Hoffman, E.J., 2001. Investigation of accelerated Monte Carlo techniques for PET simulation and 3D PET scatter correction. *IEEE Trans. Nucl. Sci.* 48 (1), 74–81. <https://doi.org/10.1109/23.910835>.
- Loudos, G.K., 2007. Monte Carlo simulations in nuclear medicine. *AIP Conf. Proc.* 958 (November 2007), 147–150. <https://doi.org/10.1063/1.2825768>.
- Martinez-Möller, A., Nekolla, S.G., 2012. Attenuation correction for PET/MR: problems, novel approaches and practical solutions. *Zeitschrift Fur Medizinische Physik* 22 (4), 299–310. <https://doi.org/10.1016/j.zemedi.2012.08.003>.
- Mohammed, M., Chakir, E., Boukhal, H., Saeed, M., El Bardouni, T., 2016. Evaluation of variance reduction techniques in BEAMnrc Monte Carlo simulation to improve the computing efficiency. *J. Radiation Res. Appl. Sci.* 9 (4), 424–430. <https://doi.org/10.1016/j.jrras.2016.05.005>.
- Musarudin, M., Saripan, M.I., Mashohor, S., Saad, W.H.M., Nordin, A.J., Hashim, S., 2015. Impact of patient weight on tumor visibility based on human-shaped phantom simulation study in PET imaging system. *Radiat. Phys. Chem.* 115 (November), 81–87. <https://doi.org/10.1016/j.radphyschem.2015.05.039>.
- Okubo, T., Endo, T., Yamamoto, A., 2017. An efficient execution of Monte Carlo simulation based on delta-tracking method using GPUs. *J. Nucl. Sci. Technol.* 54 (1), 30–38. <https://doi.org/10.1080/00223131.2016.1202793>.
- Pfaehler, E., De Jong, J.R., Dierckx, R.A.J.O., van Velden, F.H.P., Boellaard, R., 2018. SMART (SiMulation and ReconsTruction) PET: an efficient PET simulation-reconstruction tool. *EJNMMI Physics* 5 (1). <https://doi.org/10.1186/s40658-018-0215-x>.

- Raylman, R.R., Johnson, M.B., Bintrim, J., Dewasurendra, V., Crawford, K., Jaliparthi, G., Martone, P., Mantz, P., 2022. Evaluation of advanced methods and materials for construction of scintillation detector light guides. *Appl. Radiat. Isot.* 179 (May 2021), 109979 <https://doi.org/10.1016/j.apradiso.2021.109979>.
- Saeed, M., El Khoukhi, T., Boulaich, Y., Chakir, E., Maged, M., Boukhal, H., El Bardouni, T., 2016. Positron-based attenuation correction for Positron Emission Tomography data using MCNP6 code. *J. Radiation Res. Appl. Sci.* 9 (1), 101–108. <https://doi.org/10.1016/j.jrras.2015.11.002>.
- Salvadori, J., Labour, J., Odille, F., Marie, P.Y., Badel, J.N., Imbert, L., Sarrut, D., 2020. Monte Carlo simulation of digital photon counting PET. *EJNMMI Physics* 7 (1). <https://doi.org/10.1186/s40658-020-00288-w>.
- Sarrut, D., Bala, M., Bardis, M., Bert, J., Chauvin, M., Chatzipapas, K., Dupont, M., Etxebeste, A., Fanchon, L.M., Jan, S., Kayal, G., Kirov, A.S., Kowalski, P., Krzemien, W., Labour, J., Lenz, M., Loudos, G., Mehadji, B., Ménard, L., et al., 2021. Advanced Monte Carlo simulations of emission tomography imaging systems with GATE. *Phys. Med. Biol.* 66 (10) <https://doi.org/10.1088/1361-6560/abf276>.
- Shultis, J.K., Faw, R.E., 2011. *An MCNP Primer*. Kansas State University, Manhattan.
- Tan, H., Gu, Y., Yu, H., Hu, P., Zhang, Y., Mao, W., Shi, H., 2020. Total-body PET/CT: current applications and future perspectives. *Am. J. Roentgenol.* 215 (2), 325–337. <https://doi.org/10.2214/AJR.19.22705>.
- Waeleh, N., Saripan, M.I., Musarudin, M., Mashohor, S., Ahmad Saad, F.F., 2021. Modeling and experimental verification of Biograph TruePoint PET/CT using MCNP5. In: *Proceedings - 2020 IEEE EMBS Conference on Biomedical Engineering and Sciences. IECBES 2020*, pp. 319–323. <https://doi.org/10.1109/IECBES48179.2021.9398805>.
- Wang, Y., Mazur, T.R., Green, O., Hu, Y., Li, H., Rodriguez, V., Wooten, H.O., Yang, D., Zhao, T., Mutic, S., Li, H.H., 2016. A GPU-accelerated Monte Carlo dose calculation platform and its application toward validating an MRI-guided radiation therapy beam model. *Med. Phys.* 43 (7), 4040–4052. <https://doi.org/10.1118/1.4953198>.
- Xie, S., Zhang, X., Zhang, Y., Ying, G., Huang, Q., Xu, J., Peng, Q., 2020. Evaluation of various scintillator materials in radiation detector design for Positron Emission Tomography (PET). *Crystals* 10 (10), 1–15. <https://doi.org/10.3390/cryst10100869>.
- Yanagida, T., 2018. Inorganic scintillating materials and scintillation detectors. *Proc. Jpn. Acad. Ser. B Phys. Biol. Sci.* 94 (2), 75–97. <https://doi.org/10.2183/pjab.94.007>.
- Zhao, J., Liu, Q., Li, C., Song, Y., Zhang, Y., Chen, J., 2022. Optimization of spatial resolution and image reconstruction parameters for the Small-Animal Metis™ PET/CT System. *Electronics* 11 (1542), 1–13.
- Zoubair, M., Bardouni, T. El, Allaoui, O., Boulaich, Y., Bakkari, B. El, Younoussi, C. El, Boukhal, H., Chakir, E., 2013. Computing efficiency improvement in Monte Carlo simulation of a 12 MV photon beam medical LINAC. *World J. Nucl. Sci. Technol.* 14–21. <https://doi.org/10.4236/wjnst.2013.31003>, 03(01).